

An Adaptive Sampling Solution using Autonomous Underwater Vehicles

Baozhi Chen, Parul Pandey, and Dario Pompili

*Department of Electrical and Computer Engineering
Rutgers University, New Brunswick, NJ
Emails: {baozhi_chen, parul_pandey, pompili}@cac.rutgers.edu*

Abstract: To achieve efficient and cost-effective sensing coverage of the vast under-sampled 3D aquatic volume, intelligent adaptive sampling strategies involving Autonomous Underwater Vehicles (AUVs) endowed with underwater wireless (acoustic) communication capabilities are essential. These AUVs should coordinate and steer through the region of interest, and cooperatively sense, preprocess and transmit measured data to onshore stations for processing and analysis. Given a scalar field to sample, i.e., a phenomenon like temperature or salinity distribution, the AUVs should coordinate to take measurements using minimal resources (time or energy) in order to reconstruct the field with admissible error. A novel adaptive sampling solution to minimize the sampling cost is proposed, which requires the AUVs to take a small number of samples from the field. We observe via simulations that our solution outperforms existing solutions that are based on Compressive Sensing (CS) techniques.

Keywords: Adaptive Sampling; Compressive Sensing; Autonomous Underwater Vehicles.

1. INTRODUCTION

Ocean weather forecast relies on the state (such as temperature) of the fluid sampled at a given time and uses fluid dynamics and thermodynamics to predict the state of the fluid in the future [Lynch (2008)]. It is known that a small uncertainty in the initial and boundary conditions (such as ocean surface temperature) may lead to large deviation in real-time ocean forecasting [Palmer (1999)]. To minimize such deviation, an accurate reconstruction of the ocean scalar field is therefore necessary. Existing observation solutions using satellites lack depth information, whereas using static observation networks may not be optimal as sampling regions of different dynamics requires the ability to change the sensor spatial distribution. Consequently, there is a need for adaptive sampling solutions as the sensors should be deployed and moved dynamically for optimal sampling performance. This can be done using a team of Autonomous Underwater Vehicles (AUVs), which can coordinate to sample the phenomenon.

To be able to perform adaptive sampling, the AUVs need to adjust real time their trajectory, inter-vehicle distance, or formation based on the field measurements. In [Chen and Pompili (2012)], we proposed sampling of a field by a team of AUVs by controlling the group trajectory. The sampling technique employed was not adaptive but took as input information from oceanographers. Many adaptive sampling solutions for measurement of ocean physical and chemical processes using AUVs have been proposed such as [Yilmaz et al. (2008); Fiorelli et al. (2003); Popa et al. (2004)]. These solutions focus on tracking a given region in such a way as to maximize certain objective functions, e.g., the gradient of the process.

Recently, Donoho has proposed Random Compressive Sensing (RCS), which offers a novel way to capture and reconstruct a signal using minimal number of samples [Donoho (2006)]. In RCS, a sparse signal $\mathbf{x} \in \mathbb{C}^N$ with sparsity S (i.e., the number of non-zero elements in \mathbf{x}), with $S \ll N$, can be recovered from the measurement $\mathbf{y} \in \mathbb{C}^K$, where $K \geq S \cdot \log N$, by finding the solution to the following optimization problem: minimize the ℓ_1 -norm $\|\mathbf{x}\|_{\ell_1}$ subject to $\mathbf{y} = \Phi\mathbf{x}$, where Φ is the $K \times N$ *sensing* (also called *measurement*) matrix.

Another paradigm, called Deterministic Compressive Sensing (DCS) [DeVore (2007)], has been introduced where the sensing matrix Φ is constructed *deterministically* using different coding schemes, e.g., the discrete chirp codes [Applebaum et al. (2009)]. Note that, given a scalar field, RCS takes samples at *random* locations, whereas DCS takes samples at locations *pre-estimated* using coding schemes. The major drawback of these techniques is that they do not take into account the real-time characteristics of the field to estimate the locations from where samples should be taken, which makes them unsuitable to implement adaptive sampling strategies. For example, to accurately reconstruct a temperature field, regions with relatively constant (i.e., low-varying) temperature values should be sampled at a lower rate than regions with large variations in temperature. CS techniques are not able to exploit the distinction between the rate of sampling based on features from the field of interest.

For this reason, we propose a novel adaptive sampling solution for AUVs to reconstruct a scalar ocean phenomenon. We first obtain a preliminary estimate of the field using a conventional lawn-mower trajectory (Phase I) and then take samples at locations estimated by an optimization algorithm (Phase II). The objective of the optimization

* Work supported by the NSF CAREER Award No. OCI-1054234.

algorithm is: *first*, to reconstruct the phenomenon by *minimizing the maximum* reconstruction error (Sub-procedure 1); *then*, to minimize the energy consumption for one pass of sampling for long-term monitoring missions (Sub-procedure 2). Our contributions are: 1) we adaptively estimate the sampling locations in the field of interest by minimizing a cost (or utility) function that represents the reconstruction error or consumed energy (depending on the application requirements); 2) we propose a solution that allows a team of AUVs to sample *jointly* a field using our sampling solution; and 3) we compare our solution against DCS and RCS, which cannot adapt to field measurements, and show that our solution outperforms them.

The remainder of this paper is organized as follows: in Sect. 2, we describe our proposed solution to sample adaptively a region of interest; in Sect. 3, we evaluate the performance of our approach; finally, in Sect. 4, we draw the conclusions and provide a brief note on future work.

2. PROPOSED SOLUTION

To sample a field of interest, an AUV moves across a field by following a certain trajectory and takes samples as it moves. One conventional method to achieve this is to steer the AUV in a *lawn-mower style* and take samples at equidistant positions: such a method is, however, inefficient as the AUV needs to scan through the whole area. Conversely, efficient solutions can be developed that take samples at a smaller number of locations so to reduce the cost (such as energy or error) incurred to reconstruct the field. We present our solution that minimizes a cost function (energy or reconstruction error, depending on the application requirements) to sample a region of interest.

Our solution consists of two phases: **Phase I**, in which the field is scanned *completely* using conventional lawn-mower-style sampling to obtain a preliminary estimate of the field; and **Phase II**, in which the field is scanned *adaptively* after Phase I. Phase II is *repeated* until it is necessary to re-run Phase I (e.g., when the field has changed ‘appreciatively’ from its preliminary measurement of Phase I). Phase I serves as a preceding stage to collect preliminary field information for Phase II. We assume that the process to be measured in the sampling field is changing slowly so that the change of field between two consecutive rounds of Phase II is very small. Depending on the movement characteristics of the vehicles in use, different sampling strategies can be applied. For example, if the AUVs are propeller driven, the 3D region can be divided into multiple 2D horizontal planes to reduce the control complexity of changing the buoyancy or vertical thruster to move up or down. Hence, in this paper we focus on sampling a 2D horizontal plane.

2.1 Centralized Multi-Vehicle Sampling Optimization

Once the preliminary estimate of the field is obtained in Phase I, we adaptively sample the field in Phase II, which is further subdivided into two sub-procedures. Each sub-procedure aims at reconstructing the scalar field by *minimizing* a particular objective function: the maximum reconstruction error (sub-procedure 1) and the energy consumption (sub-procedure 2). The two sub-procedures

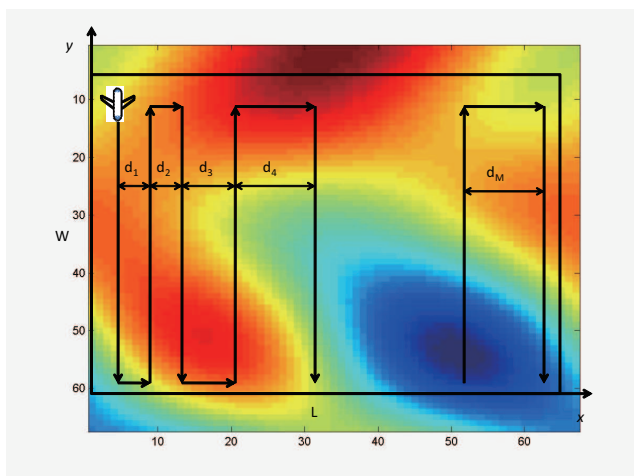


Fig. 1. Trajectory planning for one vehicle, $V = 1$.

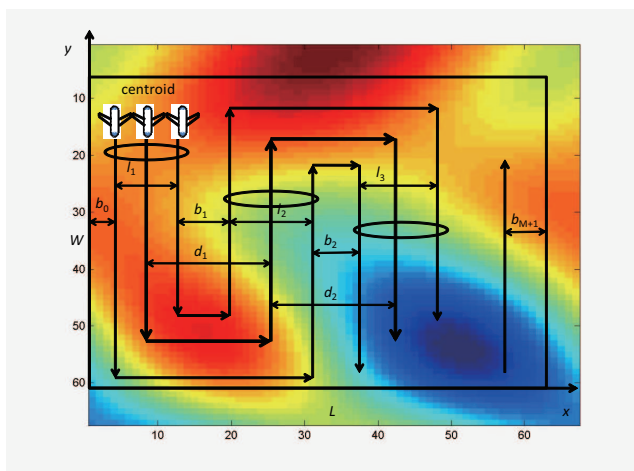


Fig. 2. Trajectory planning for three vehicles, $V = 3$.

are run *consecutively*, with sub-procedure 1 employed first to obtain accurate reconstruction of the field and later, for long-term sampling of a field, sub-procedure 2 is employed, which takes samples by minimizing the energy while the reconstruction error is bounded. Note that both sub-procedures can also be run *independently* according to the sampling mission requirement (i.e., minimizing reconstruction error or consumed energy).

To illustrate the idea of our solution, we start from the case when the number of vehicles is one, i.e., $V = 1$ (Fig. 1). The AUV will follow the lawn-mower trajectory to scan the region. At each pass of the scan, the AUV uses the field information it got from the previous scan to optimize its lawn-mower trajectory. In other words, the AUV uses the field reconstructed during the $(k - 1)^{th}$ pass to optimize its trajectory at the k^{th} pass; it calculates the optimal number M^* of segments as well as the distances d_m 's ($m = 1, \dots, M^*$) between two neighboring line segments. Further improvement can be made by using the samples collected in all previous passes to optimize the current pass. Note that during the first, i.e., the 0^{th} pass, the AUV follows a conventional lawn-mower trajectory with equal spacing, whose distance is given by oceanographers based on a-priori information on the field. Suppose the reconstructed field for the k^{th} pass is denoted by $\hat{f}_k(x, y, z)$ at

position (x, y, z) , then d_m 's should be selected to minimize the function $\max_{(x,y,z) \in \mathcal{R}} |\hat{f}_k(x, y, z) - \hat{f}_{k-1}(x, y, z)|$, where \mathcal{R} denotes the region being sampled. As shown in Fig. 1, based on the previous sampling information, the vehicle decides the optimal number M^* of segments (parallel to the y -axis) and the distances d_m 's between consecutive segments; then, it follows this optimal trajectory while sampling. Generally speaking, the reconstructed \hat{f} has a large error in regions with frequent changes as there the reconstruction is less accurate. Therefore, d_m in these regions should be small. On the other hand, the reconstructed \hat{f} has small error in regions with less changes, resulting in large d_m in these regions.

We now formulate an optimization problem for sub-procedure 1 where the maximal reconstruction error should be minimized with the energy consumption as a constraint. We assume that multiple AUVs are used to sample the field. As $V > 1$, besides M^* and the distances d_m 's between two neighboring line segments, we need to include the dimension of the whole team, as illustrated in Fig. 2 for $V = 3$. Suppose the AUVs form a linear formation of width l_m with the same distance between each pair of neighbors when they are taking samples at the m^{th} segment. We denote the margin distances of the starting and ending segments by b_0 and b_{M+1} , respectively. Similarly to the case of a single vehicle, we should optimize M , d_m 's, and l_m 's ($m = 1, \dots, M$).

Multi-Vehicle Error Minimization Problem:

$$\begin{aligned} \text{Find: } & M^*, d_m^*, l_m^*; m = 1, \dots, M^* \\ \text{Min: } & \max_{(x,y,z) \in \mathcal{R}} |\hat{f}_k(x, y, z) - \hat{f}_{k-1}(x, y, z)| \\ \text{S.t.: } & E_j(S, M, v) = E_{seg,j}(S, v) + E_{turn,j}(\theta_m) + N_{smp} E_{smp,j}; \\ & E_j(S, M, v) \leq E_{th}. \end{aligned} \quad (1)$$

In this formulation, $\hat{f}_k(x, y, z)$ denotes the reconstructed field value at position (x, y, z) for the k^{th} pass, l_m is the group width of these V AUVs. $E_{seg,j}(S, v)$, $E_{turn,j}(\theta_m)$, and $E_{smp,j}$ are the energy consumed while vehicle j travels through the line segments, makes turns, and takes one sample, respectively. Besides the energy consumption, the AUVs are constrained by the time constraint to finish one pass and by the dimension of the sampling field.

Additional Relations and Constraints:

$$\sum_{m=1}^M d_m + (l_1 + l_M)/2 + b_0 + b_{M+1} \leq L; \quad (3)$$

$$S = M \cdot W + \sum_{m=1}^{M-1} d_m; \quad (4)$$

$$d_m = (l_m + l_{m-1})/2 + b_m; \quad (5)$$

$$b_m = l_m/(V-1); \quad (6)$$

$$t_j(S, M, v) = \frac{S}{v} + \sum_{m=1}^M t_j(\theta_m) + N_{smp} t_{smp,j}; \quad (7)$$

$$t_j(S, M, v) \leq T_{th}; \quad (8)$$

$$d_m \geq d_{th}; \quad (9)$$

$$b_0 \leq l_1/(V-1); \quad b_{M+1} \leq l_M/(V-1). \quad (10)$$

Here, (4) represents the total length of the trajectory given the width of the field W and the distance between two neighboring segments d_m . The distance between segments

of team of AUVs is represented by (5) given the number of vehicles V and width of linear formation l_m of the team of AUVs, while (7) represents the time taken to finish one round of sampling given the time taken to turn $t_j(\theta_m)$, number of samples N_{smp} taken by the team of AUV, and velocity v of the team of AUVs. Constraint (8) imposes that the time taken to finish one round of sampling be below a threshold value, whereas (9) constraints the distance between two neighboring segments d_m be greater than a pre-defined threshold value d_{th} . In (10) the maximum value of margin distance of the starting and ending segments of AUVs is defined given number of vehicles V and number of segments M .

For sub-procedure 2, we change the objective function to be the minimization of the energy to finish one pass of sampling and add an error bounding constraint, leading to the following optimization problem.

Multi-Vehicle Energy Minimization Problem:

$$\begin{aligned} \text{Find: } & M^*, d_m^*, l_m^*; m = 1, \dots, M^* \\ \text{Min: } & E_j(S, M, v); \\ \text{S.t.: } & \max_{(x,y,z) \in \mathcal{R}} |\hat{f}_k(x, y, z) - \hat{f}_{k-1}(x, y, z)| \leq \epsilon. \end{aligned} \quad (11)$$

While executing a particular sub-procedure, the vehicles send their samples to one vehicle, called *team leader*. This leader then estimates the field of interest $\hat{f}(x, y, z)$ using methods such as interpolation/extrapolation. For example, if bilinear interpolation is used to estimate a 2D field, the value at (x, y) can be represented by $\hat{f}(x, y) = \frac{1}{x_{i+1}^k - x_i^k} \cdot \frac{1}{y_{j+1}^k - y_j^k} \cdot [x_{i+1}^k - x \quad x - x_i^k] \cdot \mathbf{A}_{i,j}^k \cdot [y_{j+1}^k - y \quad y - y_j^k]^T$, where (x, y) is in the region constrained by $[x_i^k, x_{i+1}^k]$ along the x -axis and $[y_j^k, y_{j+1}^k]$ along the y -axis, $\mathbf{A}_{i,j}^k$ is the 2×2 measurement matrix at the k^{th} round, i.e., $\mathbf{A}_{i,j}^k = [\hat{f}(x_i^k, y_j^k) \quad \hat{f}(x_{i+1}^k, y_j^k); \hat{f}(x_i^k, y_{j+1}^k) \quad \hat{f}(x_{i+1}^k, y_{j+1}^k)]$. From (9) and (8), we can estimate the range of M being $M \leq \min(L/d_{th}, T_{th} \cdot v/W)$. To solve it, we can do the exhaustive search after discretization, i.e., d_m and l_m can only take one value in the set $\{m \cdot L/N_L, m = 0, \dots, N_L - 1\}$ of N_L numbers, whose computation complexity is $\mathcal{O}(M_{\min} \cdot N_L^{M_{\min}})$, where $M_{\min} = \min(L/d_{th}, T_{th} \cdot v/W)$. Improvements to such search can be made by observing the specific characteristics of the field $\hat{f}(x, y, z)$.

2.2 Distributed Multi-Vehicle Sampling Optimization

To reduce the complexity of the above optimization at the leader side, the computation can be distributed to the whole team of AUVs. To achieve this, we can decompose the centralized optimization problem into sub-problems that can be run at different AUVs. We can discretize the x direction into H_x values, which is then further partitioned into V intervals. These intervals are then distributed to the V vehicles of the team and each vehicle will estimate the team trajectory in its assigned interval. In this way, the problem can be decomposed into sub-optimization problems for individual vehicles to solve. Note that the boundaries of these sub-problems should be the same for consecutive regions, i.e., the ending point of one region should be the same as the starting point of the next region. Each vehicle solves for the same optimization for their assigned sub-region. In addition, we add two more

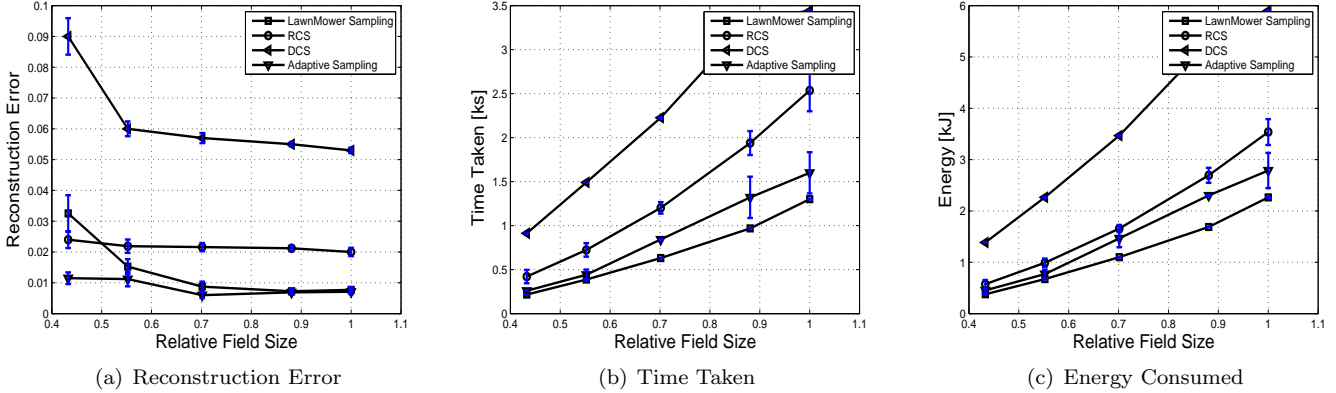


Fig. 3. Performance comparison of our solution with existing sampling solutions.

constraints for the starting and ending point of the planned trajectory – the starting point of the trajectory in one sub-region should be the same as the ending point in its previous sub-region, and the ending point should be the same as the starting point in its next sub-region. *These two constraints introduce coupling between consecutive sub-problems.* Such coupling can be removed by adding an interface variable representing the constrained position between two consecutive sub-problems. After the assigned sub-problem is solved, each vehicle sends the optimal parameters and trajectory back to the team leader so that the trajectory for the whole region is obtained.

3. PERFORMANCE EVALUATION

We compared via thorough simulations our sampling solutions against 1) the conventional lawn-mower-style sampling (which is based on the AUV-coordination solution proposed in [Chen and Pompili (2012)], where the AUVs follow a lawn-mower trajectory and take measurements equidistant from each other), 2) DCS (where the sampling locations are chosen using discrete chirp codes [Applebaum et al. (2009)]), and 3) RCS (which is based on [Hummel et al. (2011)], where measurements are taken at random locations in the field). For both RCS and DCS, once the locations have been determined *offline*, a shortest-path algorithm is run to calculate the trajectory of AUVs.

We present the results for both proposed sub-procedures; the metrics for comparison are: i) *minimum reconstruction error*, ii) *energy consumed*, and iii) *time taken* to sample the field. We assumed the temperature field is a unit 2D square (i.e., $1 \times 1 \text{ km}^2$) region on the ocean surface. Each AUV is assumed to move at a horizontal speed of 0.001 unit distance per second (e.g., 1 m/s in a $1 \times 1 \text{ km}^2$ region). The communication between AUVs is assumed to use *ideal underwater acoustic technology* (i.e., no errors and no delay). For statistical relevance, we ran simulations over 50 different ocean temperature images and the average is plotted with 95% confidence intervals. The images used for simulation are accessible at [JPL (2012)].

We first present the results for sub-procedure 1 of our solution in comparison to existing solutions in Fig. 3(a). For Phase I of sub-procedure 1, we use a lawn-mower trajectory to obtain a preliminary estimate of the field. This estimate is also required by DCS and RCS to construct

the measurement matrix. Lawn-mower-style sampling does not require preliminary estimate of the field as it takes samples at equidistant locations in the original field. We see that our solution gives minimum reconstruction error in comparison to other techniques. The main reason for this is that existing solutions do not consider the characteristics of the field of interests to estimate the sampling locations. They select fixed number of samples irrespective of the underlying data, hence, are not adaptive to field measurements. The DCS solution, which uses chirp codes, requires that the sparsity be much higher than that present in the temperature images considered in our simulations, as a result of which the reconstruction error is high.

Figure 3(b) shows the time taken by the vehicle to sample a field versus the size of the region. The time taken is calculated as the sum of time taken to do the pre-scanning in Phase 1 and to acquire samples at locations provided by different techniques. Compared to DCS, our solution takes shorter time because it requires fewer samples for reconstruction. The time taken by our solution is higher than that by lawn-mower-style sampling as we employ a pre-scanning phase to get a preliminary estimate of the field. The pre-scanning phase is not included in lawn-mower-style sampling.

For sub-procedure 2, the energy is calculated by bounding the reconstruction error of the field obtained in sub-procedure 1. Figure 3(c) shows the energy consumed while sampling the field versus the variation in field size. We see that our solution consumes lower energy than DCS because fewer measurements are required. The energy consumed by our solution is comparable to that by RCS. As our solution involves an additional pre-scanning phase, the energy consumed by our solution is higher than that by the lawn-mower style sampling in spite of having almost equal number of measurements in Phase II.

In Figs. 4(a),(b),(c) and Figs. 5(a),(b), we present an example of a reconstructed field using our adaptive sampling solution and other existing solutions (the sampling locations in the field are denoted by white dots). In Fig. 5(b), we can see that – although our solution follows a trajectory similar to a conventional lawn-mower technique – the samples are not equidistant from each other, i.e., they are chosen adaptively by our optimization algorithm.

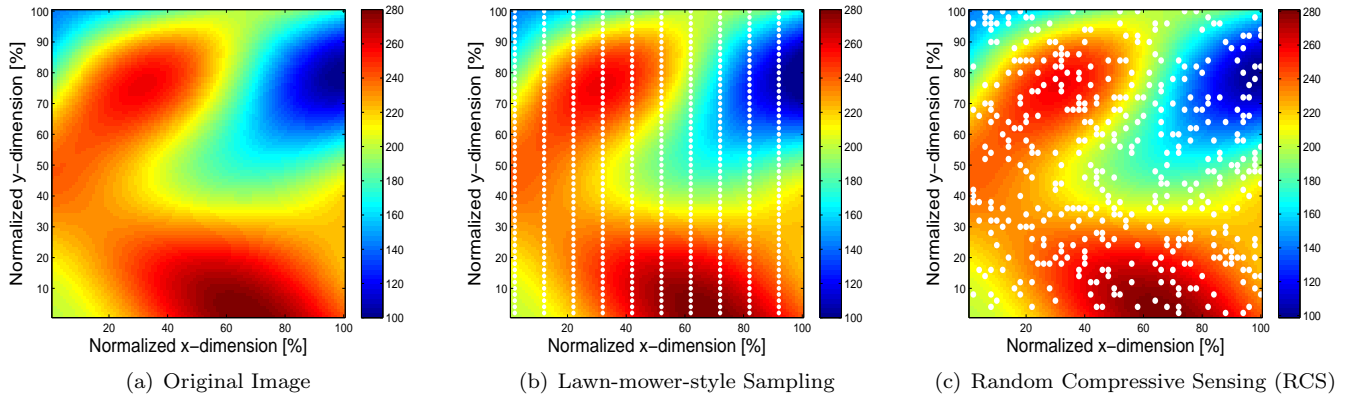


Fig. 4. Reconstructed images with sampling locations (denoted by white dots).

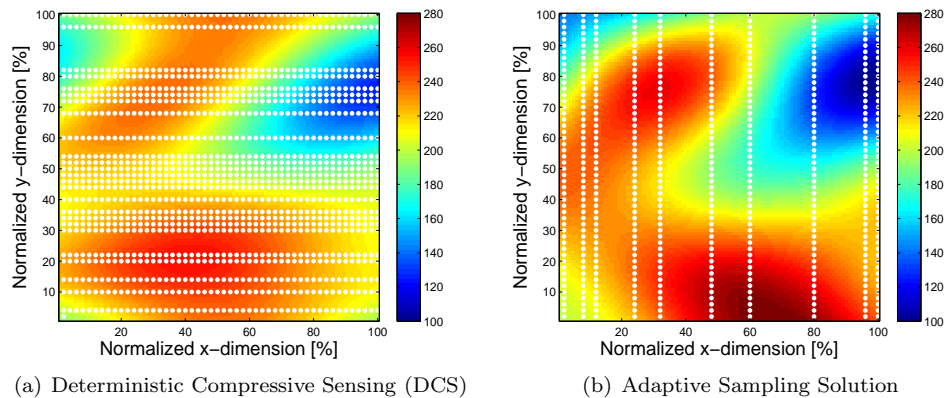


Fig. 5. Reconstructed images with sampling locations (denoted by white dots).

4. CONCLUSION AND FUTURE WORK

We proposed an adaptive sampling solution for a team of Autonomous Underwater Vehicles (AUVs) to sample the ocean temperature field and developed efficient distributed algorithms that can minimize the sampling cost (energy or time). These solutions minimize a cost (or utility) function that represents the reconstruction error or the consumed energy to sample a phenomenon. Our solution is compared against existing sampling solutions and improved performance is observed. As future work, we will extend our solution to fast-changing phenomena by incorporating the prediction for the change of the sampled phenomenon.

REFERENCES

- Applebaum, L., Howard, S., Searle, S., and Calderbank, R. (2009). Chirp sensing codes: Deterministic compressed sensing measurements for fast recovery. *Applied and Computational Harmonic Analysis (Elsevier)*, 26(2), 283–290.
- Chen, B. and Pompili, D. (2012). Team Formation and Steering Algorithms for Underwater Gliders using Acoustic Communications. *Computer Communication (Elsevier)*, 35, 1017–1028.
- DeVore, R.A. (2007). Deterministic Constructions of Compressed Sensing Matrices. *Journal of Complexity (Elsevier)*, 23, 918–925.
- Donoho, D.L. (2006). Compressed Sensing. *IEEE Transactions on Information Theory*, 52, 1289–1306.
- Fiorelli, E., Bhatta, P., and Leonard, N.E. (2003). Adaptive sampling using feedback control of an autonomous underwater glider fleet. In *Proc. of International Symposium on Unmanned Untethered Submersible Technology*.
- Hummel, R., Poduri, S., Hover, F., Mitra, U., and Sukhatme, G. (2011). Mission design for compressive sensing with mobile robots. In *Proc. of IEEE International Conference on Robotics and Automation (ICRA)*.
- JPL (2012). OurOcean Portal, California Institute of Technology. <http://ourocean.jpl.nasa.gov/>.
- Lynch, P. (2008). The origins of computer weather prediction and climate modeling. *Journal of Computational Physics (Elsevier)*, 227, 3431–3444.
- Palmer, T.N. (1999). Predicting uncertainty in forecasts of weather and climate. *European Centre for Medium-Range Weather Forecasts (ECMWF) Technical Memorandum*, 294.
- Popa, D.O., Sanderson, A.C., Komerska, R., Mupparapu, S., Blidberg, R., and Chappel, S. (2004). Adaptive Sampling Algorithms for Multiple Autonomous Underwater Vehicles. In *Proc. of IEEE/OES on Autonomous Underwater Vehicles*.
- Yilmaz, N.K., Evangelinos, C., Lermusiaux, P.F.J., and Patrikalakis, N.M. (2008). Path Planning of Autonomous Underwater Vehicles for Adaptive Sampling Using Mixed Integer Linear Programming. *IEEE Journal of Oceanic Engineering*, 33(4), 522–537.